JPET Fast Forward. Published on January 25, 2007 as DOI:10.1124/jpet.106.116954

JPET #116954

Activation by Zonisamide, a Newer Anti-Epileptic Drug, of Large-Conductance Calcium-Activated Potassium Channel in Differentiated Hippocampal Neuron-Derived H19-7 Cells

Chin-Wei Huang, Chao-Ching Huang, and Sheng-Nan Wu

Department of Neurology (C.W.H.) and Institute of Clinical Medicine (C.W.H., C.C.H.), Department of Pediatrics (C.C.H.), Department of Physiology and Institute of Basic Medical Sciences (S.N.W.), National Cheng Kung University Medical College, Tainan, Taiwan

Running title: Zonisamide action in hippocampal neurons

Address correspondence to: Dr. Sheng-Nan Wu, Department of Physiology, National Cheng Kung University Medical College, No. 1, University Road, Tainan 70101, Taiwan. Tel: 886-6-2353535-5334; Fax: 886-6-2353660; e-mail: snwu@mail.ncku.edu.tw

Number of text pages: 32

Number of tables: 1

Number of figures: 8

Number of references: 40

Number of words in

Abstract: 235

Introduction: 575

Discussion: 712

Abbreviations: **ZNS**: zonisamide; $\mathbf{BK_{Ca}}$: large-conductance Ca^{2+}-activated K^+; $\boldsymbol{I_K}$: K^+ Outward Currents; $\boldsymbol{I_{Ca,L}}$**: L-type** $\mathbf{Ca^{2+}}$ **Current**; $\boldsymbol{I_A}$:A-Type K^+ Current; $\boldsymbol{I_{Na}}$:Na^+ current; ***I-V***: the current-voltage relations

Section: Neuropharmacology

Abstract

Zonisamide (ZNS), 3-sulfamoylmethyl-1,2-benzisoxazole, as one of the newer antiepileptic drug, has been demonstrated its broad-spectrum clinical efficacy on various neuropsychiatric disorders. However, little is known regarding the mechanism of ZNS actions on ion currents in neurons. We thus investigated its effect on ion currents in differentiated hippocampal 19-7 cells. In whole-cell configuration of patch clamp technology, the ZNS (30 μM) reversibly increased the amplitude of K^+ outward currents, and paxilline (1 μM) was effective in suppressing the ZNS-induced increase of K^+ outward currents. In inside-out configuration, ZNS (30 μM) applied to the intracellular face of the membrane did not alter single-channel conductance; however, it did enhance the activity of large-conductance Ca^{2+}-activated K^+ (BK_{Ca}) channels primarily by decreasing mean closed time. In addition, the EC_{50} value for ZNS-stimulated BK_{Ca} channels was 34 μM. This drug caused a left shift in the activation curve of BK_{Ca} channels with no change in the gating charge of these channels. Moreover, ZNS at a concentration greater than 100 μM also reduced the amplitude of A-type K^+ current in these cells. A simulation modeling based on hippocampal CA3 pyramidal neurons (Pinsky-Rinzel model) was also analyzed to investigate the inhibitory effect of ZNS on the firing of simulated action potentials. Taken together, this study suggests that in hippocampal neurons, during the exposure to ZNS, the ZNS-mediated effects on BK_{Ca} channels and I_A could be potential mechanisms through which it affects neuronal excitability.

Introduction

Zonisamide (ZNS) is a benzisoxazole derivative with a non-arylamine sulphonamide group and is chemically unrelated to other antiepileptic drugs. It has been characterized as having broad-spectrum antiepileptic and neuroprotective effects (Leppik, 2004; Baulac, 2006). Previous reports have demonstrated the ability of this drug to block voltage-dependent Na^+ channels and T-type Ca^{2+} channels (Schauf, 1987; Suzuki et al., 1992; Leppik, 2004). It also has been shown to inhibit the ryanodine-induced increase in basal levels of glutamate and GABA in the rat hippocampus (Yoshida et al., 2005). In addition, ZNS has been reported as potentially blocking glutamate activity in the frontal cortex (Huang et al., 2005) and the firing of action potentials in spinal cord neurons (Rock et al., 1989). A recent report showed that ZNS could improve depressive symptoms in acute bipolar depression (Ghaemi et al., 2006). However, the mechanisms through which this drug can halt seizures or modulate mood activity are largely unknown, despite its increased use in the treatment of epilepsy or biopolar disorders.

The large-conductance Ca^{2+}-activated K^+ (BK_{Ca}) channels, the products of a nearly ubiquitous, alternatively spliced gene (*SLO or KCNMA1*) (Butler et al., 1993), are distinguished from other K^+ channels in that they are gated open in response to Ca^{2+} binding to sites located inside of the channel, as well as by depolarized membrane potentials (Ghatta et al., 2006; Wu et al., 2006). Their activities provide a link between the metabolic and electrical state of cells, because they are sensitive to stimulation by increased intracellular Ca^{2+}. BK_{Ca} channels in hippocampal pyramidal cells have been identified for their collaborative effect with voltage-gated K channels in repolarizing spike and fast afterhyperpolarization (Storm et al., 1990; Shao et al., 1999). Besides, riluzole and cilostazol have been reported to enhance the

activity of BK_{Ca} channels in pituitary tumor (GH_3) cells (Wu et al., 1999, 2004).

A recent study has demonstrated that mutation of the pore-forming α-subunit of BK_{Ca} channels could cause generalized epilepsy, paroxysmal dyskinesia (Du et al., 2005) and mental deficiency disorder such as autism (Laumonnier et al., 2006). In addition, the increased activity of BK_{Ca} channels, possibly associated with the peripheral antinociceptive action of metamizol and meloxicam (Ortiz et al., 2003; 2005), could counteract the deleterious effects of excitatory neurotransmitters following neurotoxic or ischemic injuries as well (Gribkoff et al., 2001; Ghatta et al., 2006). However, it remains unknown whether ZNS, as a potential neuropsychiatric modulator, produces any effects on the activity of these channels.

The hippocampal neuron-derived H19-7 cell line is known to possess the characteristics of hippocampal neurons (Morrione et al., 2000; Bhargava et al., 2002). This cell line has been used for studies on the development, plasticity, and commitment in hippocampal neurons (Morrione et al., 2000; Bhargava et al., 2002). Therefore, the goal of this study is as follows: 1) to examine the effect of ZNS on K^+ outward current in differentiated hippocampal H19-7 cells, 2) address the issue of whether this drug can affect the activity and kinetic properties of BK_{Ca} channels, and 3) determine whether it affects other types of ion currents present in these cells. Interestingly, these results indicate that ZNS can directly enhance the activity of BK_{Ca} channels.

Methods

Cell Preparation

The H19-7 cell line was originally derived from hippocampi dissected from embryonic day 17 Holtzman rat embryos and immortalized by retroviral transduction of temperature sensitive tsA58 SV40 large T antigen. This cell line was obtained from American Type Culture Collection ([CRL-2526], Manassas, VA) (Morrione et al., 2000; Huang et al., 2004). Cells were maintained in Dulbecco's modified Eagle's media with 4 mM L-glutamine adjusted to contain 1.5 g/l sodium bicarbonate and 4.5 g/l glucose supplemented with 10% fetal bovine serum, 200 μg/ml G418 and 1 μg /ml puromycin in flasks that were coated with 15 μg/ml poly-L-lysine. They were equilibrated in a humidified atmosphere of 5% CO_2/95% at an air temperature with a permissive temperature of 34 °C. The experiments were generally performed after 5 days of subcultivation (60-80% confluence) with cells obtained from passages 2 and 4.

Cell Differentiation

For differentiation experiments, hippocampal H19-7 cells were plated at a density of 10^5 cells/35-mm plate in a medium containing serum at 34 °C. After 18 hr, the cells were washed extensively and then shifted to a non-permissive temperature (39 °C) in N2 SFM (i.e., DMEM-high glucose medium supplemented with 0.11 mg/ml sodium pyruvate, 2 mM glutamine, 0.1 mg/ml transferrin, 20 nM progesterone, 0.1 mM putrescine, and 30 nM sodium selenite), supplemented with 50 ng/ml IGF-I (Life Technologies, Grand Island, NY). After 48 hr, the cells were harvested and observed for neurite formation and subsequent electrophysiological experiments (Kim et al., 1997; Morrione et al., 2000). Therefore, rat hippocampal neurons-derived H19-7 cells could either proliferate at the permissive temperature of 34 °C in response

to insulin-like growth factor, or differentiate to a neuronal phenotype in N2 medium at the non-permissive temperature of 39 °C (Kim et al., 1997; Morrione et al., 2000; Huang et al., 2006).

Electrophysiological Measurements

Immediately before each experiment, differentiated H19-7 cells were dissociated, and an aliquot of cell suspension was transferred to a recording chamber positioned on the stage of an inverted microscope (DM IL; Leica Microsystems, Wetzlar, Germany). Cells were bathed at room temperature (20-25 °C) in normal Tyrode's solution containing 1.8 mM $CaCl_2$. The recording pipettes were pulled from Kimax-51 glass capillaries (Kimble Glass, Vineland, NJ) using a two-stage microelectrode puller (PP-830; Narishige, Tokyo, Japan), and the tips were fire-polished with a microforge (MF-83; Narishige). When filled with pipette solution, their resistance ranged between 3 and 5 MΩ. Ion currents were recorded in a whole-cell or inside-out configuration of the patch-clamp technique, using an RK-400 patch-clamp amplifier (Bio-Logic, Claix, France) (Huang et al., 2006). All potentials were corrected for liquid junction potential, a value that would always develop at the tip of the pipette when the composition of the pipette solution was different from that in the bath. Tested drugs were applied through perfusion or added to the bath to obtain the final concentration indicated.

Data Recordings and Analyses

The signals consisting of voltage and current tracings were displayed on an analog/digital oscilloscope (HM 507; Hameg Inc., East Meadow, NY). The data were stored on-line in a laptop computer through an analog/digital interface (Digidata 1322A; Molecular Devices, Union City, CA), controlled by a commercially-available software package (pCLAMP 9.0; Molecular Devices). The sampling rate for

electrophysiological measurements was 10 kHz. Currents were low-pass filtered at 1 or 3 kHz. Ion currents recorded during experiments were stored and analyzed subsequently using pCLAMP 9.0 software (Molecular Devices), Origin 7.5 software (Microcal Software, Inc., Northampton, MA), SigmaPlot 7.0 software (SPSS, Inc., Apex, NC), or custom-made macros in Excel 2003 (Microsoft, Redmond, WA). The pCLAMP-generated voltage-step protocols were generally used to examine the current-voltage (*I-V*) relations for ion currents.

To calculate concentration-dependent stimulation of ZNS on the activity of BK_{Ca} channels, H19-7 cells were bathed in a high-K^+ (145 mM) solution, and inside-out configuration was performed. Each excised patch was held at +60 mV, and the bath medium contained 0.1 μM Ca^{2+}. The concentration-dependent effect of ZNS at different concentrations (3-100 μM) was fitted with a Hill function. That is, relative open probability = $(E_{max} \times [C]^{n_H}) / (EC_{50}{}^{n_H} + [C]^{n_H})$, where [C] represents the ZNS concentration; n_H and EC_{50} are Hill coefficients, and the ZNS concentration needed to increase channel activity by 50%, respectively; and E_{max} is the ZNS-induced maximal stimulation of BK_{Ca} channels.

Single-channel currents of BK_{Ca} or K_{ATP} channels were analyzed using pCLAMP 9.0 software (Molecular Devices). Multi-gaussian adjustments of the amplitude distributions between channels were used to determine unitary currents. The functional independence between channels was verified by comparing the observed stationary probabilities with the values calculated according to binomial law. The number of active channels in the patch N was counted at the end of each experiment and then used to normalize opening probability at each potential. The open probabilities were evaluated using an iterative process to minimize the χ^2 calculated with a sufficiently large number of independent observations. The open or closed

distribution of the channel was fit with a one- or two-exponential function.

The plots of the open probability of BK_{Ca} channels as a function of membrane potential were constructed and fit with a Boltzmann function using nonlinear regression analysis with the Origin 7.5 (Microcal). That is, relative open probability $= n_p/\{1 + \exp[-(V - V_{1/2})/k]\}$, where n_p = the maximal probability of channel openings, V = the membrane potential in mV, $V_{1/2}$ = the membrane potential for half-maximal activation, and *k* = the slope factor of the activation curve.

The averaged results are presented as the mean values ± S.E.M. The paired or unpaired *t* test and one-way ANOVA with the least significance difference method for multiple comparisons were used for statistical evaluation of the differences among the mean values. Differences between values were considered significant when $p < .05$ or $< .01$.

Drugs and Solutions

Zonisamide (1,2-benzisoxazole-3-methanesulfonamide; Zonegran®) was kindly provided from Dainippon Pharmaceuticals (Osaka, Japan). Riluzole (2-amino-6-trifluoromethoxybenzothiazole) was obtained from Tocris Cookson Ltd. (Bristol, UK). Tetraethylammonium chloride and tetrodotoxin were purchased from Sigma Chemical (St. Louis, MO), apamin and iberiotoxin were from Alomone Labs (Jerusalem, Israel), and paxilline was from Biomol (Plymouth Meeting, PA) (Wu et al., 2006). All other chemicals were commercially available and of reagent grade. The twice-distilled water that had been de-ionized through a Millipore-Q system was used in all experiments.

The composition of normal Tyrode's solution was 136.5 mM NaCl, 5.4 mM KCl, 1.8 mM $CaCl_2$, 0.53 mM $MgCl_2$, 5.5 mM glucose, and 5.5 mM HEPES-NaOH buffer, pH 7.4. To record K^+ currents, patch pipette was filled with a solution consisting of

140 mM KCl, 1 mM $MgCl_2$, 3 mM Na_2ATP, 0.1 mM Na_2GTP, 0.1 mM EGTA, and 5 mM HEPES-KOH buffer, pH 7.2. To record Ca^{2+} current, KCl inside the pipette solution was replaced with equimolar CsCl, and pH was adjusted to 7.2 with CsOH. In single-channel recordings, high K^+-bathing solution contained 145 mM KCl, 0.53 mM $MgCl_2$, and 5 mM HEPES-KOH, pH 7.4, and the pipette solution contained 145 mM KCl, 2 mM $MgCl_2$, and 5 mM HEPES-KOH, pH 7.2.

Mathematical Modeling

Spontaneous discharge of neurons was simulated using the model of hippocampal CA3 pyramidal neurons, which was originally derived from Pinsky and Rinzel (1994). The important role of CA3 neurons in kindling and temporal lobe seizures has been established (Jang et al., 2006). This model consists of a fast and transient Na^+ current, a persistent, depolarization-activated Na^+ current, a low-threshold Ca^{2+} current, a high-threshold Ca^{2+} current, a Ca^{2+}-activated K^+ current, a transient outward K^+ current, a slowly inactivating K^+ current, and a hyperpolarization-activated cation current. The source file for this model is readily available at http://cams.njit.edu/~vbooth/. The solutions to the different sets of ordinary differential equations in the simulations were approximated using the X-Win32 version of XPPAUT on a Dell Precision 670 workstation (Round Rock, TX) (Ermentrout 2003; Wu and Chang 2006).

Results

Stimulatory Effect of ZNS on K^+ Outward Currents (I_K) in Differentiated Hippocampal H19-7 Cells

In the initial set of experiments, the whole-cell configuration of the patch-clamp technique was used to investigate the effect of ZNS on macroscopic I_K. When H19-7 cells were bathed in normal Tyrode's solution containing 1.8 mM $CaCl_2$, I_K in response to a 1-sec long ramp pulse could be elicited. This current was found to be outwardly rectifying. Within 1 min of exposing the cells to ZNS (30 μM), the amplitude of I_K evoked by the ramp pulse was significantly increased (Figure 1). For example, at the level of +80 mV, ZNS (30 μM) significantly increased the amplitude of I_K from 795 ± 59 to 1509 ± 74 pA ($p < .05$, n = 6). In addition, ZNS (30 μM) increased the slope conductance of I_K at the level of +40 mV from 16.7 ± 2.3 nS (n = 5) to 24.2 ± 3.5 nS (n = 5), and at the level of +80 mV from 18.4 ± 2.5 to 35.7 ±3.6 nS (n=5). After washout of ZNS, the amplitude of I_K returned to 822 ± 31 pA (n = 5). A further application of 1 μM paxilline could reduce I_K to 812 ± 63 pA ($p < .05$, n = 5). In addition, iberiotoxin (200 nM), but not apamin (200 nM), significantly reversed the ZNS-induced increase of I_K. In addition, the value for reversal potential of I_K measured in the presence of ZNS or ZNS plus paxilline was around -75 mV. The results suggest that the amplitude of I_K in response to the ramp pulses can be sensitive to increases in ZNS. The ZNS-induced increase of I_K can be blocked by paxilline or iberiotoxin.

Stimulatory Effect of ZNS on the Activity of BK_{Ca} Channels in Differentiated H19-7 Cells

Paxilline and iberiotoxin, known inhibitors of BK_{Ca} channels, could reverse ZNS-stimulated I_K. The increased macroscopic I_K could be due to the increased

open probability, an increase in the number of active channels, or both. The effect of ZNS on BK_{Ca}-channel activity in these cells was further investigated (Figure 2). In these experiments, single-channel recordings with an inside-out configuration were performed in symmetrical K^+ solution (145 mM) (Figure 2A). Bath medium contained 0.1 μM Ca^{2+}, and holding potential was held at +60 mV. When ZNS (100 μM) was applied to the intracellular surface of the excised patch, the channel activity was significantly increased to 0.015 ± 0.004 (n = 5) from a control of 0.004 ± 0.001 (n = 5, $p < .05$). A further application of paxilline (1 μM) could decrease the channel activity to 0.005 ± 0.001 (n = 5). The channel activity in paxilline (1 μM) alone was 0.003 ± 0.001(n = 5). Application of ZNS (3-1000 μM) was found to enhance the probability of channel openings in a concentration-dependent manner. The half-maximal concentration required for the stimulatory effect of ZNS on BK_{Ca}-channel activity was 34 μM, and Hill coefficient was 1.2. Thus, the ZNS-induced increase in the amplitude of I_K in these cells could be associated with its increase in the open probability of BK_{Ca} channels, rather than changes in the number of active channels.

Lack of Effect of ZNS on Single-Channel Conductance of BK_{Ca} Channels

In the next series of experiments, the effect of ZNS on single-channel conductance was investigated. In inside-out configuration, the cells were bathed in symmetrical K^+ solution (145 mM), and the bath medium contained 0.1 μM Ca^{2+}. Figure 3A illustrates averaged *I-V* relationships of BK_{Ca} channels obtained in the absence and presence of ZNS (30 μM). The single BK_{Ca} channel conductance calculated from a linear *I-V* relationship in control (i.e., in the absence of ZNS) was 166 ± 11 pS (n = 8) with a reversal potential of 0 ± 2 mV (n = 8). The value of single-channel conductance was not found to differ significantly from that (168 ± 10

pS; (n = 8), $p > .05$) measured during the exposure to ZNS (30 μM). These results indicate that this drug does not cause any modification in single-channel conductance, despite its ability to increase the open probability of these channels.

Effect of ZNS on the Activation Curve of BK_{Ca} Channels

Figure 3B shows the activation curve of BK_{Ca} channels in the absence and presence of ZNS (30 μM). The plot of open probability of channel openings as a function of membrane potential was fitted with a Boltzmann function as described under "Materials and Methods". In control, $n_p = 1$, $V_{1/2} = 56 \pm 5$ mV, and $k = 11.6 \pm 2.1$ mV (n =6), whereas in the presence of ZNS (100 μM), $n_p = 1.6 \pm 0.2$, $V_{1/2} = 42 \pm 6$ mV, and $k = 11.5 \pm 1.9$ mV (n = 6). The data thus indicate that the ZNS-increased channel activity can be accompanied by a significant shift of the steady-state activation toward less positive potentials, although the slope factor of activation curve remained unaltered. Taken together, ZNS applied to the intracellular surface of the channel is capable of affecting the activation curve with no change in the gating charge of these channels.

Effect of Internal Ca^{2+} Concentrations on ZNS-stimulated BK_{Ca}-Channel Activity

We next examined whether the ZNS-induced increase in the activity of these channels is associated with the level of internal Ca^{2+} concentrations. In these experiments, when an excised patch was formed, various concentrations of Ca^{2+} in the bath before and during exposure to ZNS (30 μM) were applied. As shown in Figure 3C, the extent of ZNS-stimulated BK_{Ca} channels was not altered by changes in the level of intracellular Ca^{2+} concentration. For example, at the level of +60 mV, ZNS (30 μM) increased the open probability at an internal Ca^{2+} concentration of 0.1, 1 and 10 μM to a similar magnitude (i.e., 1.6-fold).

Effect of ZNS on Kinetic Behavior of BK_{Ca} Channels in Differentiated H19-7 Cells

The effect of ZNS on mean open and closed time of BK_{Ca} channels in these cells was examined and analyzed during recordings from patches showing only single-channel openings. As shown in Figure 4, in control cells, the closed time histogram of BK_{Ca} channels at +60 mV can be fitted by a two-exponential function with a mean closed time of 5.2 ± 0.9 and 54.5 ± 1.6 msec (n = 5). ZNS (30 μM) decreased the lifetime of the closed time to 3.2 ± 0.8 and 19.6 ± 1.1 msec (n = 5, $p < .05$). However, no change in the component of open time distribution was observed in the presence of ZNS (30 μM) [1.62 ± 0.05 versus 1.64 ± 0.04 msec (n = 5), $p > .05$]. Taken together, the data suggest that the stimulation by this drug of BK_{Ca} channels in these cells is largely due to an increase in open probability accompanied by the decreased closed time.

Effect of Riluzole on BK_{Ca} Channels in Differentiated Hippocampal H19-7 Cells

Riluzole has been previously reported as stimulating BK_{Ca} channels (Wu et al., 1999). We also examined whether the stimulatory effects of ZNS and riluzole on these channels are additive. Interestingly, as shown in Figure 5, riluzole (30 μM) increased the channel open probability; however, a subsequent application of ZNS (30 μM) did not increase the channel activity further. Riluzole (30 μM) significantly increased the probability of channel openings from 0.12 ± 0.02 to 0.24 ± 0.03 (n = 6, $p < .05$). There was no significant difference in channel activity between the presence of riluzole alone and ZNS plus riluzole [0.24 ± 0.03 (n = 6) versus 0.23 ± 0.03 (n = 6), $p > .05$]. However, application of cilostazol (30 μM) could increase the open probability further when ZNS or riluzole was continuously present in the bath. Cilostazol was reported as an opener of BK_{Ca} channels (Hong et al., 2003; Wu et al.,

2004). Taken together, the results led us to suggest that riluzole potentially occluded the effect of zonisamide, although these two drugs can be effective in enhancing channel activity.

Effect of ZNS on Voltage-Dependent L-type Ca^{2+} Current ($I_{Ca,L}$) in Differentiated H19-7 Cells

The question may arise whether a ZNS-induced increase in whole-cell I_K is associated with an increased Ca^{2+} influx through voltage-dependent Ca^{2+} channels. ZNS has been previously reported as blocking Ca^{2+} current (Suzuki et al., 1992). The effect of ZNS on the amplitude of $I_{Ca,L}$ in differentiated H19-7 cells was thus assessed. In these experiments, cells were bathed in normal Tyrode's solution containing 1.8 mM $CaCl_2$ and the recording pipettes were filled with Cs^+-containing solution. Cell exposure to ZNS (30 μM) did not affect the peak amplitude of $I_{Ca,L}$. However, ZNS at a concentration of 300 μM resulted in a decrease in $I_{Ca,L}$ (Figure 6). For example, when cells were depolarized from -50 to 0 mV, the peak amplitude of $I_{Ca,L}$ was slightly but significantly decreased from 85 ± 12 to 79 ± 11 pA (n = 5, $p < .05$). In addition, a further application of nifedipine (0.3 μM), a known blocker of $I_{Ca,L}$, almost abolished the amplitude of $I_{Ca,L}$. Thus, the results indicate that this drug can stimulate Ca^{2+}-activated K^+ current in a manner unlikely to be associated with an increase in the amplitude of $I_{Ca,L}$.

Effect of ZNS on Rapidly Inactivating A-Type K^+ Current (I_A) in Differentiated H19-7 Cells

Previous studies at our laboratory have demonstrated that lamotrigine, another antiepileptic drug, could block I_A in these cells in a concentration- and state-dependent manner (Huang et al., 2004). In this study, we further examined whether ZNS causes any effect of I_A. As shown in Figure 7, ZNS at a concentration

of 100 or 300 μM could block the amplitude of I_A significantly. When the cells were exposed to ZNS, the amplitude of I_A was suppressed throughout the entire voltage clamp step. The averaged *I-V* relations for the peak amplitude of I_A in the absence and presence of ZNS are shown in Figure 7B. The results indicate that ZNS at a concentration greater than 100 μM is able to block I_A in these cells.

Effects of ZNS on Repetitive Firing of Action Potentials in Modeled Hippocampal CA3 Pyramidal Neurons

In order to determine how ZNS alters the discharge pattern of hippocampal neurons and to address questions that are difficult to be experimentally studied, a simulation model, originally derived from Pinsky and Rinzel (1994), was also implemented. ZNS has been previously reported to block voltage-dependent Na^+ current (I_{Na}) (Schauf, 1987; Leppik, 2004). In this modeled neuron, when the I_{Na} conductance was decreased from 18 to 17 nS, the peak amplitude of I_{Na} was readily reduced, along with the decreased firing of action potentials (Figure 8A). When the conductance of Ca^{2+}-activated K^+ current was increased from 20 to 40 nS, the frequency of action potential firing was further reduced (Figure 8B). As a result, the reduced I_{Na} and the increased Ca^{2+}-activated K^+ current, which mimics the ZNS action, can combine to cause a reduction in the firing of neuronal action potentials. The simulation results can be used to predict that the activity of BK_{Ca} channels could contribute to the electrical behavior of hippocampal neurons.

Discussion

The major findings of this study are as follows. First, in differentiated hippocampal H19-7 cells, ZNS, a newer antiepileptic drug, increased the amplitude of K^+ outward current. Second, ZNS increased the activity of BK_{Ca} channels in a concentration-dependent fashion with no change in single-channel conductance. Third, this drug had no effect on the open time but decreased the time constants of the closed time, thereby increasing the open probability of BK_{Ca} channels. Fourth, a high concentration of ZNS could block the amplitude of I_A. Fifth, the simulation model predicted that the decreased conductance of I_{Na} and the increased conductance of Ca^{2+}-activated K^+ current, which mimics ZNS action, could decrease the firing of action potentials in modeled hippocamal neurons. The effects on ion channels could be important mechanisms underlying ZNS-induced action.

The concentration-dependent stimulation of BK_{Ca}-channel activity with an EC_{50} value of 34 μM was observed in the presence of ZNS. This concentration of ZNS is compatible to clinically relevant concentrations, ranging from 50 to 200 μM (Peters and Sorkin, 1993; Tasaki et al., 1995; Oommen and Mathews, 1999; Huang et al., 2005). The observed effect of ZNS in this study is likely to occur at a concentration achievable in humans. It is thus reasonable to assume that BK_{Ca} channels present in neurons are a relevant 'target' for the action of ZNS. The ability of ZNS to activate BK_{Ca} channels may constitute an important component regulating neuronal function, aiding in understanding the broad-spectrum efficacy in epilepsy and various neuropsychiatric disorders.

Our study demonstrates that ZNS does not modify single-channel conductance of BK_{Ca} channels, although it increases the channel open probability significantly. The increased amplitude of macroscopic I_K is thought to be primarily due to the increased

probability of channel openings accompanied by a decrease in mean closed time. In addition, when applied to the internal face of the membrane, it did not merely increase the activity of BK_{Ca} channels in the patch, but also increased a shift of voltage sensitivity of the channel to less positive potentials. The sensitivity to this drug in neurons would be thus expected to depend on the preexisting level of resting potential, the firing rate of action potentials, or the ZNS concentration used.

It is noteworthy that unlike the molecule of cilostazol, ZNS was found to possess an intramolecular hydrogen bond with a short inter-atomic distance and an aromatic ring poor of electrons, the properties of which are shared by other inhibitors of carbonic anhydrase (Tricarico et al., 2004). The present results also demonstrate that the stimulatory effect of ZNS and riluzole on the activity of BK_{Ca} channels is not additive. Riluzole has been previously reported as an opener of BK_{Ca} channels in pituitary tumor (GH_3) cells (Wu and Li 1999). It is likely that these two components, which are structurally related, may interact with the same binding site in the channel.

Previous reports have shown that some of the indole diterpenes, which are potent inhibitors of BK_{Ca} channels, are associated with their tremorgenic activity (Knaus et al., 1994; Smith et al., 1997). Recent reports have demonstrated that as compared to β blocker, zonisamide is effective in treating essential tremor (Morita et al., 2005; Ondo, 2006). Further studies are needed to determine the extent to which ZNS-stimulated activity of BK_{Ca} channels contribute to its treatment of essential tremor.

ZNS at a concentration greater than 100 μM was found to block I_A in differentiated hippocampal H19-7 neurons. Lack of A-type K^+ channels has been proposed to decrease the seizure threshold in the cortical malformation of methylazoxymethanol-exposed rats (Castro et al., 2001). Though no report on

ZNS-worsening seizures has been noted, ZNS has been recently reported to improve depressive symptoms in bipolar disorders (Ghaemi et al., 2006). Whether its inhibition of the I_A channels has potential psychotropic benefits in treating underlying cellular disturbances in bipolar disorders, as described previously, remains to be further clarified.

Our simulation results also imply that both blockade of I_{Na} and direct stimulation of BK_{Ca} channels caused by ZNS may synergistically act to affect the functional activity of hippocampal neurons *in vivo*. Taken together, in addition to the blockade of I_{Na}, our results lead us to suggest that ZNS-mediated antiepileptic action could be partly associated with the direct stimulation of BK_{Ca} channels expressed in hippocampal neurons.

Acknowledgements

The authors would like to thank Dr. Okada Motohiro, Hirosaki University, Japan for comments on zonisamide pharmacology. The authors would also like to thank Ming-Wei Lin for technical assistance.

References

Bailey MA, Cantone A, Yan Q, MacGregor GG, Leng Q, Amorim JB, Wang T, Hebert SC, Giebisch G and Malnic G (2006) Maxi-K channels contribute to urinary potassium excretion in the ROMK-deficient mouse model of Type II Bartter's syndrome and in adaptation to a high-K diet. *Kidney Int* 70:51-59.

Baulac M (2006) Introduction to zonisamide. *Epilepsy Res* 68S:S3-S9.

Butler A, Tsunoda S, McCobb DP, Wei A and Salkoff L (1993) mSlo, a complex mouse gene encoding "maxi" calcium-activated potassium channels. *Science* 261:221-224.

Castro PA, Cooper EC, Lowenstein DH and Baraban SC (2001) Hippocampal heterotopia lack functional Kv4.2 potassium channels in the methylazoxymethanol model of cortical malformation and epilepsy. *J Neurosci* 21:6626-6634.

Du W, Bautista JF, Yang H, Diez-Sampedro A, You SA, Wang L, Kotagal P, Luders HO, Shi J, Cui J, Richerson GB and Wang QK (2005) Calcium-sensitive potassium channelopathy in human epilepsy and paroxysmal movement disorder. *Nat Genet* 37:733-738.

Ermentrout GB (2002) *Simulating, Analyzing, and Animating Dynamical System: A Guide to XPPAUT for Researchers and Students.* Society for Industrial and Applied Mathematics (SIAM), Philadelphia.

Ghaemi SN, Zablotsky B, Filkowski MM, Dunn RT, Pardo TB, Isenstein E and Baldassano CF (2006) An open prospective study of zonisamide in acute bipolar depression. *J Clin Psychopharmacol* 26:385-388.

Ghatta S, Nimmagadda D, Xu XP and O'Rourke ST (2006) Large-conductance, calcium-activated potassium channels: structural and functional implications.

Pharmacol Ther 110:103-116.

Gribkoff VK, Starrett JE Jr, Dworetzky SI, Hewawasam P, Boissard CG, Cook DA, Frantz SW, Heman K, Hibbard JR, Huston K, Johnson G, Krishnan BS, Kinney GG, Lombardo LA, Meanwell NA, Molinoff PB, Myers RA, Moon SL, Ortiz A, Pajor L, Pieschl RL, Post-Munson DJ, Signor LJ, Srinivas N, Taber MT, Thalody G, Trojnacki JT, Wiener H, Yeleswaram K and Yeola SW (2001) Targeting acute ischemic stroke with a calcium-sensitive opener of maxi-K potassium channels. *Nat Med* 7:471-477.

Hong KW, Kim KY, Shin HK, Lee JH, Choi JM, Kwak YG, Kim CD, Lee WS and Rhim BY (2003) Cilostazol prevents tumor necrosis factor-α-induced cell death by suppression of phosphatase and tension homolog deleted from chromosome 10 phosphorylation and activation. *J Pharmacol Exp Ther* 306:1182-1190.

Huang CW, Huang CC, Liu YC and Wu SN (2004) Inhibitory effect of lamotrigine on A-type potassium current in hippocampal neuron-derived H19-7 cells. *Epilepsia* 45:729-736.

Huang CW, Ueno S, Okada M and Kaneko S (2005) Zonisamide at clinically relevant concentrations inhibits field EPSP but not presynaptic fiber volley in rat frontal cortex. *Epilepsy Res* 67:51-60.

Huang CW, Huang CC and Wu SN (2006) The opening effect of pregabalin on ATP-sensitive potassium channels in differentiated hippocampal neuron-derived H19-7 cells. *Epilepsia* 47:720-726.

Jang IS, Nakamura M, Ito Y and Akaike N (2006) Presynaptic GABAa receptors facilitate spontaneous glutamate release from presynaptic terminals on mechanically dissociated rat CA3 pyramidal neurons. *Neuroscience* 138:25–35.

Kim B, Leventhal PS, Saltiel AR and Feldman EL (1997) Insulin-like growth

factor-I-mediated neurite outgrowth in vitro requires mitogen-activated protein kinase activation. *J Biol Chem* 272:21268-21273.

Knaus HG, McManus OB, Lee SH, Schmalhofer WA, Garcia-Calvo M, Helms LM Sanchez M, Giangiacomo K, Reuben JP and Smith AB 3rd (1994) Tremorgenic indole alkaloids potently inhibit smooth muscle high-conductance calcium-activated potassium channels. *Biochemistry* 33:5819-5828.

Laumonnier F, Roger S, Guerin P, Molinari F, M'rad R, Cahard D Belhadj A, Halayem , Persico AM, Elia M, Romano V, Holbert S, Andres C, Chaabouni H, Colleaux L, Constant J, Le Guennec JY and Briault S (2006). Association of a functional deficit of the BK_{Ca} channel, a synaptic regulator of neuronal excitability, with autism and mental retardation. *Am J Psychiatry* 163:1622-1629.

Leppik IE (2004) Zonisamide: chemistry, mechanism of action, and pharmacokinetics. *Seizure* 13:S5-S9.

Morita S, Miwa H and Kondo T (2005) Effect of zonisamide on essential tremor: a pilot crossover study in comparison with arotinolol. *Parkinsonism Relat Disord* 11:101-103.

Morrione A, Romano G, Navarro M, Reiss K, Valentinis B, Dews M, Eves E, Rosner MR and Baserga R (2000) Insulin-like growth factor I receptor signaling in differentiation of neuronal H19-7 cells. *Cancer Res* 60:2263-2272.

Ondo WG (2006) Essential tremor: treatment options. *Curr Treat Options Neurol* 8:256-267.

Oommens KJ and Mathews S (1999) Zonisamide: a new anti-epileptic drug. *Clin Neuropharmacol* 22:192-200.

Ortiz MI, Castañeda-Hernández G and Granados-Soto V (2003) Possible involvement

of potassium channels in peripheral antinociception induced by metamizol: lack of participation of ATP-sensitive K^+ channels. *Pharmacol Biochem Behav* 74:465-470.

Ortiz MI, Castañeda-Hernández G and Granados-Soto V (2005) Pharmacological evidence for the activation of Ca^{2+}-activated K^+ channels by meloxicam in the formalin test. *Pharmacol Biochem Behav* 81:725-731.

Peters DH and Sorkin EM (1993) Zonisamide. A review of its pharmacodynamic and pharmacokinetic properties, and therapeutic potential in epilepsy. *Drugs* 45:760-787.

Pinsky PF and Rinzel J (1994) Intrinsic and network rhythmogenesis in a reduced Traub model for CA3 neurons. *J Comput Neurosci* 1:39-60.

Rock DM, Macdonald RL and Taylor CP (1989) Blockade of sustained repetitive action potentials in cultured spinal cord neurons by zonisamide (AD 810, CI 912), a novel anticonvulsant. *Epilepsy Res* 3:138-143.

Schauf CL (1987) Zonisamide enhances slow sodium inactivation in *Myxicola*. *Brain Res* 413:185-188.

Shao LR, Halvorsrud R, Borg-Graham L and Storm JF (1999) The role of BK-type Ca^{2+}-dependent K^+ channels in spike broadening during repetitive firing in rat hippocampal pyramidal cells. *J Physiol* 521:135-146.

Smith BL, McLeay LM and Embling PP (1997) Effect of the mycotoxins penitrem, paxilline and lolitrem B on the electromyographic activity of skeletal and gastrointestinal smooth muscle of sheep. *Res Vet Sci* 62:111-116.

Storm JF (1990) Potassium currents in hippocampal pyramidal cells. *Prog Brain Res* 83:161-187.

Suzuki S, Kawakami K, Nishimura S, Watanabe Y, Yagi K, Seino M and Miyamoto

K (1992) Zonisamide blocks T-type calcium channel in cultured neurons of rat cerebral cortex. *Epilepsy Res* 12:21-27.

Tanabe M, Sakaue A, Takasu K, Honda M and Ono H (2005) Centrally mediatedd antihyperalgesic and antiallodynic effects of zonisamide following partial nerve injury in the mouse. Naunyn-Schmiedebergs *Arch Pharmacol* 372:107-114.

Tasaki K, Minami T, Ieiri I, Ohtsubo K, Hirakawa Y, Ueda K, Higuchi S (1995) Drug interactions of zonisamide with phenytoin and sodium valproate: serum concentrations and protein binding. *Brain Dev* 17:182-185.

Tricarico D, Barbieri M, Mele A, Carbonara G and Camerino DC (2004) Carbonic anhydrase inhibitors are specific openers of skeletal muscle BK channel of K^+-deficient rats. *FASEB J* 18:760-761.

Wu SN and Chang HD (2006) Diethyl pyrocarbonate, a histidine-modifying agent, directly stimulates activity of ATP-sensitive potassium channels in pituitary GH_3 cells. *Biochem Pharmacol* 71:615-623.

Wu SN and Li HF (1999) Characterization of riluzole-induced stimulation of large-conductance calcium-activated potassium channels in rat pituitary GH_3 cells. *J Invest Med* 47:484-495.

Wu SN, Liu SI and Huang MH (2004) Cilostazol, an inhibitor of type 3 phosphodiesterase, stimulates large-conductance, calcium-activated potassium channels in pituitary GH_3 cells and pheochromocytoma PC12 cells. *Endocrinology* 145:1175-1184.

Wu SN, Wu AZ and Lin MW (2006) Pharmacological roles of the large-conductance calcium-activated potassium channel. *Curr Top Med Chem* 6:1025-1030.

Yoshida S, Okada M, Zhu G and Kaneko S (2005) Effects of zonisamide on neurotransmitter exocytosis associated with ryanodine receptors. *Epilepsy Res*

67:153-162.

Footnotes

This work was supported by grants from the National Science Council (NSC-94-2320B-006-019, NSC-94-2314-B-006-040, NSC-95-2314-B-006-046, and NSC-95-2745-B006-002-MY2), Taiwan and the Program for Promoting Academic Excellence & Developing World Class Research Centers, Ministry of Education, Taiwan.

Reprint requests: Dr. Sheng-Nan Wu, Department of Physiology, National Cheng Kung University Medical College, No. 1, University Road, Tainan 70101, Taiwan. Tel: 886-6-2353535-5334; Fax: 886-6-2353660; e-mail: snwu@mail.ncku.edu.tw

Legends for Figures

Figure 1. Effect of ZNS on K^+ outward current (I_K) in differentiated H19-7 cells. In these experiments, cells were bathed in normal Tyrode's solution containing 1.8 mM $CaCl_2$ and $CdCl_2$ (0.5 mM). Each cell was held at -50 mV, and the ramp pulses from -80 to +100 mV with a duration of 1 sec were applied. (**A**) Original current traces showing the effect of ZNS on I_K obtained with or without a further application of paxilline. ZNS: zonisamide (30 μM); Pax: paxilline (1 μM). (**B**) Bar graph showing the effect of ZNS on I_K in the absence and presence of paxilline, iberiotoxin, or apamin. The amplitude was measured at the level of +80 mV. ZNS: zonisamide (30 μM); Pax: paxilline (1 μM); Iber: iberiotoxin (200 nM); Apa: apamin (200 nM). Each point represents the mean ± S.E.M. (n = 4-9). $^{*}p < .05$ versus control. $^{**}p < .05$ versus ZNS alone group.

Figure 2. Stimulatory effect of ZNS on BK_{Ca}-channel activity in differentiated H19-7 cells. (A) Each excised patch was held at +60 mV. Channel activity during the exposure to ZNS (1 mM) was taken to be 1.0, and those at different concentrations of ZNS were then compared. (B) The relationship between the ZNS concentration and BK_{Ca}-channel activity. The red smooth line represents the best fit to the Hill equation. The values for EC_{50} and the Hill coefficient were 34 μM and 1.2, respectively. (C) Bar graph showing the effect of ZNS, ZNS with addition of Pax and Pax alone on I_K. Each point represents the mean ± S.E.M. (n = 5-10). $^{*}p < .05$ versus control. $^{**}p < .05$ versus ZNS alone group. Pax: paxilline (1 μM).

Figure 3. Effect of ZNS on the *I-V* relationship and the Ca^{2+}-sensitivity of BK_{Ca} channels in differentiated H19-7 cells. Experiments in excised patches were

conducted in symmetrical K^+ solution (145 mM) and a bath medium containing 0.1 μM Ca^{2+}. (**A**) Averaged *I-V* relationship of BK_{Ca} channels in the absence (■) and presence (□) of 100 μM ZNS. Data are the mean ± SEM (n = 6-10). Notably, there is no significant change in single-channel conductance between the absence and presence of ZNS. (**B**) Relationships between membrane potential and the open probability of BK_{Ca} channels obtained in the absence (■) and presence (□) of 30 μM ZNS. Data are the mean ± S.E.M. (n = 5-8). (**C**) Lack of ZNS effect on Ca^{2+} sensitivity of BK_{Ca} channels. Potential was held at +60 mV, and various concentrations of Ca^{2+} in the bath were applied before and during exposure to ZNS (30 μM). Data are the mean ± S.E.M. (n = 4-6). *Significantly different from controls (i.e., in the absence of ZNS) ($p < .05$).

Figure 4. Effect of ZNS on mean open (upper) and closed (lower) time of BK_{Ca} channels in differentiated H19-7 cells. Inside-out configuration was performed in these experiments, and the potential was held at +60 mV. Cells were bathed in symmetrical K^+ solution (145 mM), and bath medium contained 0.1 μM Ca^{2+}. The open (upper) and closed (lower) time histograms after application of ZNS are shown in the right. Control data were obtained from measuring 296 channel openings with a total record time of 1 min, whereas those obtained in the presence of ZNS were measured from 339 channel openings with a total record time of 30 sec. The red dashed lines shown in each lifetime distribution are placed at the values of the time constant in an open or closed state.

Figure 5. Effects of riluzole, ZNS, riluzole plus ZNS, ZNS plus cilostazol, and riluzole plus cilostazol on the activity of BK_{Ca} channels. Channel activity of each

excised patch was measured at +60 mV. ZNS: 30 μM zonisamide; Ril: 30 μM riluzole; Cil: 30 μM cilostazol. In the experiments with ZNS or riluzole plus cilostazol, cilostazol was subsequently applied in the continued presence of ZNS or riluzole. Each point represents the mean ± S.E.M. (n= 5-9). *Significantly different from control group. **Significantly different from ZNS alone group. ***Significantly different from the riluzole alone group.

Figure 6. Inhibitory effect of ZNS on voltage-dependent L-type Ca^{2+} current ($I_{Ca,L}$) in differentiated H19-7 cells. In these experiments, the cells were bathed in normal Tyrode's solution that contained 1.8 mM $CaCl_2$, 1 μM tetrodotoxin, and 10 mM tetraethylammonium chloride. The recording pipettes were filled with a Cs^+-containing solution. (**A**) Original currents showing the effects of ZNS and ZNS plus nifedipine on $I_{Ca,L}$. The cell was depolarized from -50 to 0 mV at a rate of 0.05 Hz. (**B**) Bar graph showing the effect of ZNS on the amplitude of $I_{Ca,L}$ with or without addition of nifedipine. ZNS: zonisamide (300 μM); Nif: nifedipine (0.3 μM). *Significantly different from control ($p < .05$). **Significantly different from the ZNS alone group ($p < .05$).

Figure 7. Inhibitory effect of ZNS on I_A in differentiated H19-7 cells. Cells were bathed in Ca^{2+}-free solution containing tetrodotoxin (1 μM) and $CdCl_2$ (0.5 mM). (A) Original current traces showing the effect of ZNS (100 and 300 μM) on I_A in these cells. The cells were depolarized from -50 to +50 mV with a duration of 300 msec. (B) Averaged *I-V* relationships of I_A in the absence (■) and presence (□) of ZNS. Each point represents the mean ± S.E.M. (n = 5-7).

Figure 8. Simulation modeling used to mimic ZNS effects on repetitive firing of action potentials in hippocampal neurons. The model was developed based on the electrophysiological properties of hippocampal CA3 pyramidal neurons as described in "Materials and Methods". In (**A**), when the I_{Na} conductance was arbitrarily decreased from 18 to 17 nS, the amplitude of I_{Na} was readily reduced, together with the decrease in the firing of neuronal action potentials. In (**B**), when the conductance of Ca^{2+}-activated K^+ current was increased from 20 to 40 nS in the continued presence of reduced I_{Na} conductance, which resembles the effects of ZNS, the action potential firing frequency was further reduced, together with the increased amplitude of Ca^{2+}-activated K^+ current in this modeled neuron. The horizontal bar shown in each panel indicates the reduction of I_{Na} conductance in combination with or without increased conductance of Ca^{2+}-activated K^+ current.

Table 1

Table 1-Default parameters values used for the modeling of hippocampal CA3 pyramidal neurons

Symbol	Description	Value
Cm	Membrane capacitance	3 μF
g_{Na}	Na^+ current conductance	18 nS
g_{Kdr}	Delayed rectifier K^+ current conductance	15 nS
g_{Ca}	Ca^{2+} current conductance	1 nS
g_{Kahp}	After-hyperpolarization K^+ current conductance	0.8 nS
g_{KCa}	Ca^{2+}-activated K^+ current conductance	20 nS
g_{Katp}	ATP-sensitive K^+ current conductance	0.3 nS
V_{Ca}	Ca^{2+} reversal potential	+80 mV
V_{Na}	Na^+ reversal potential	+60 mV
V_K	K^+ reversal potential	-75 mV

Figure 1

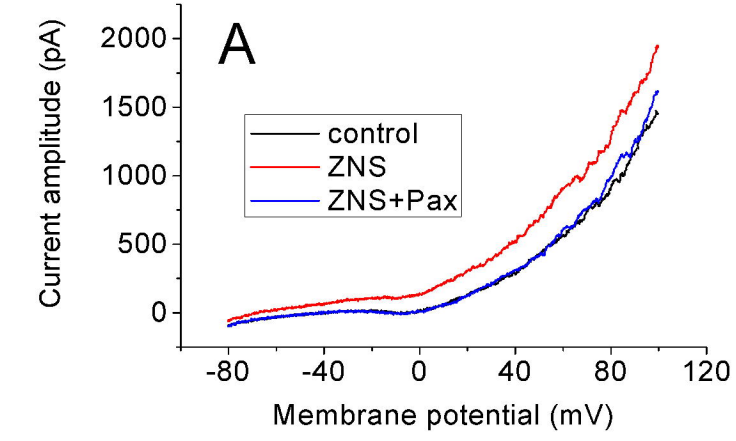
A
Current amplitude (pA)
2000
1500
1000
500
0
control
ZNS
ZNS+Pax
-80
-40
0
40
80
120
Membrane potential (mV)

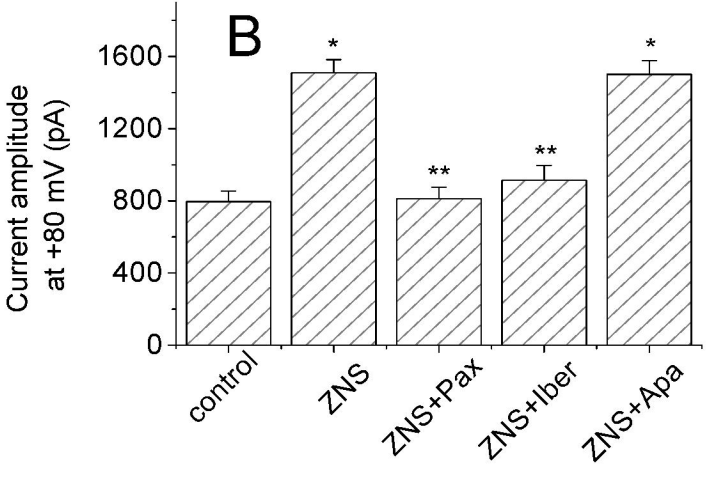
B
Current amplitude at +80 mV (pA)
1600
1200
800
400
0
*
**
**
*
control
ZNS
ZNS+Pax
ZNS+Iber
ZNS+Apa

Figure 2

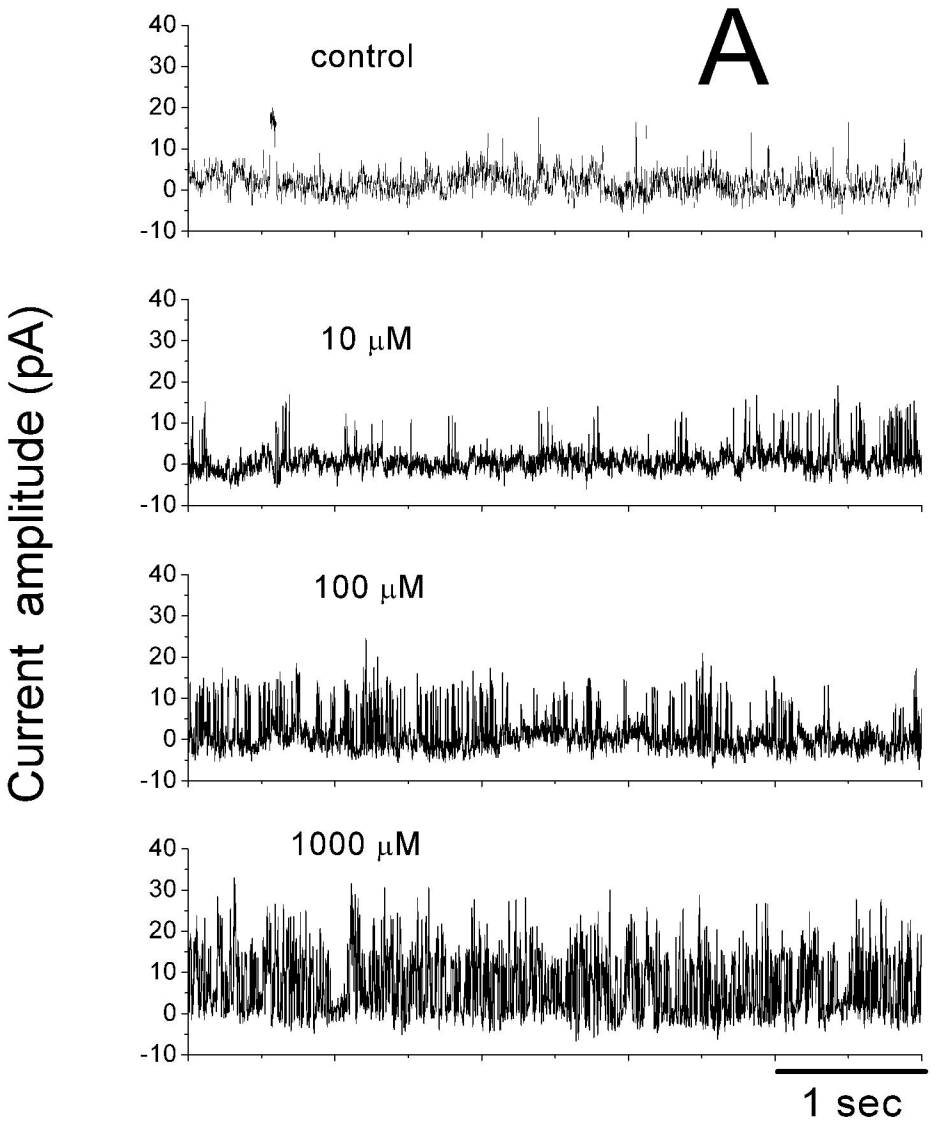
A
control
10 μM
100 μM
1000 μM
40
30
20
10
0
-10
Current amplitude (pA)
1 sec

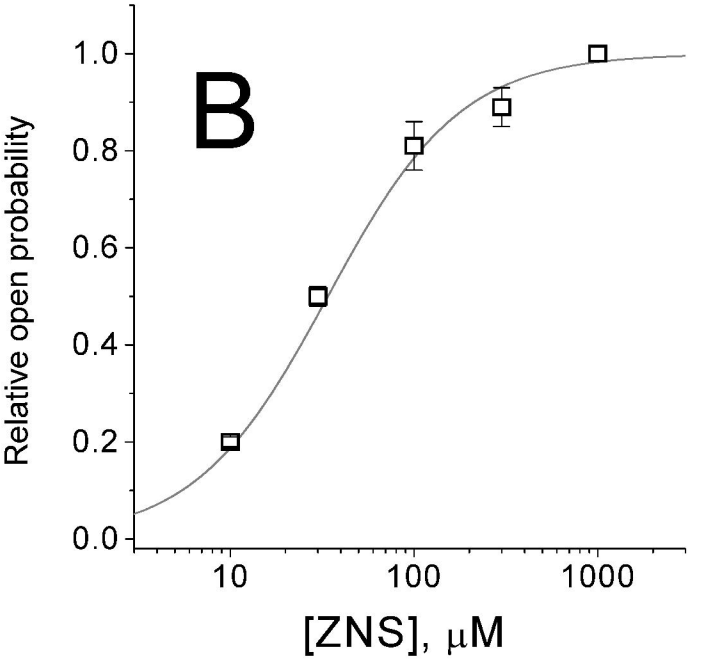
B
Relative open probability
1.0
0.8
0.6
0.4
0.2
0.0
10
100
1000
[ZNS], μM

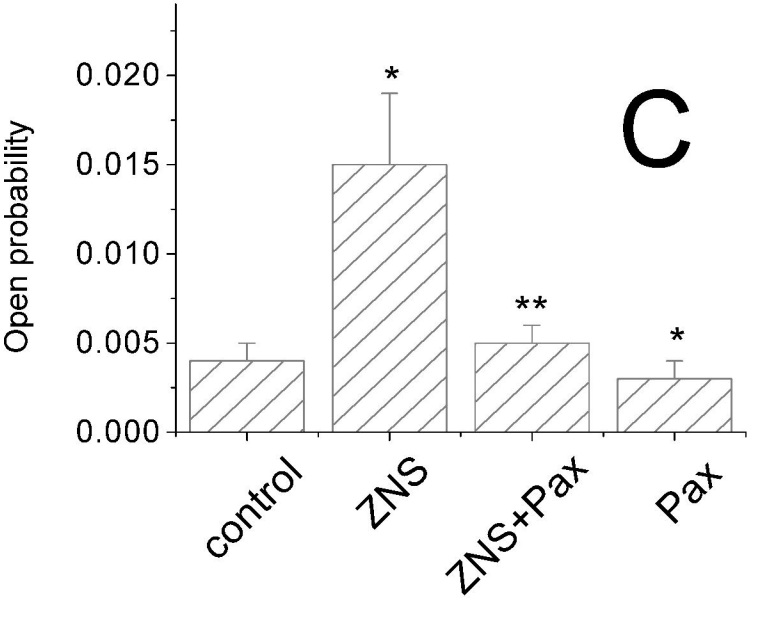
C
Open probability
0.020
0.015
0.010
0.005
0.000
*
**
*
control
ZNS
ZNS+Pax
Pax

Figure 3

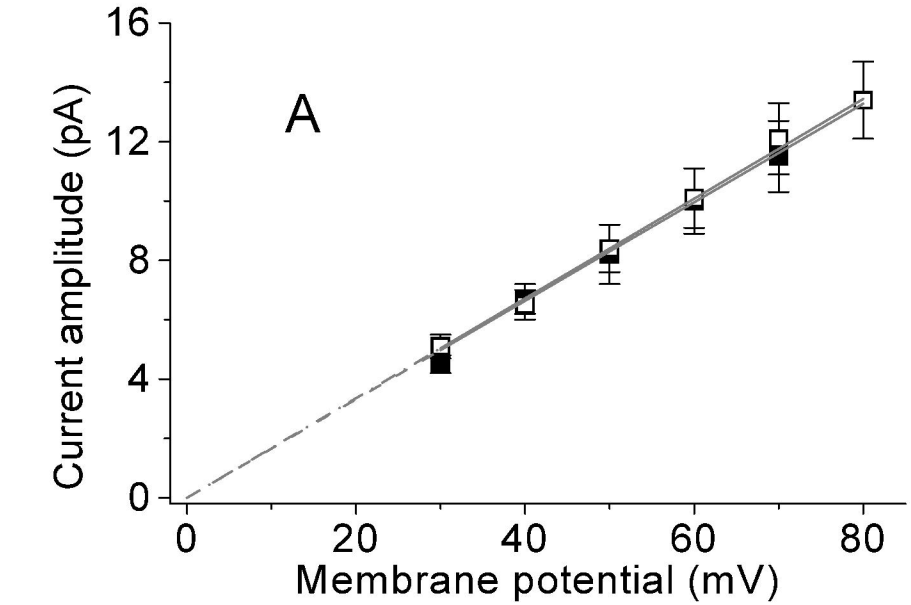
A
Current amplitude (pA)
Membrane potential (mV)
0
4
8
12
16
0
20
40
60
80

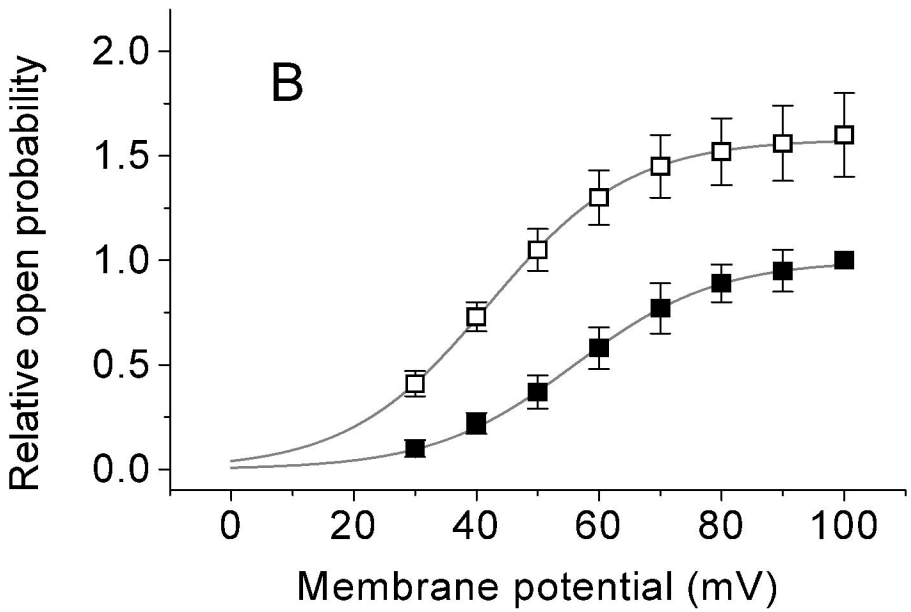
B
Relative open probability
Membrane potential (mV)
0.0
0.5
1.0
1.5
2.0
0
20
40
60
80
100

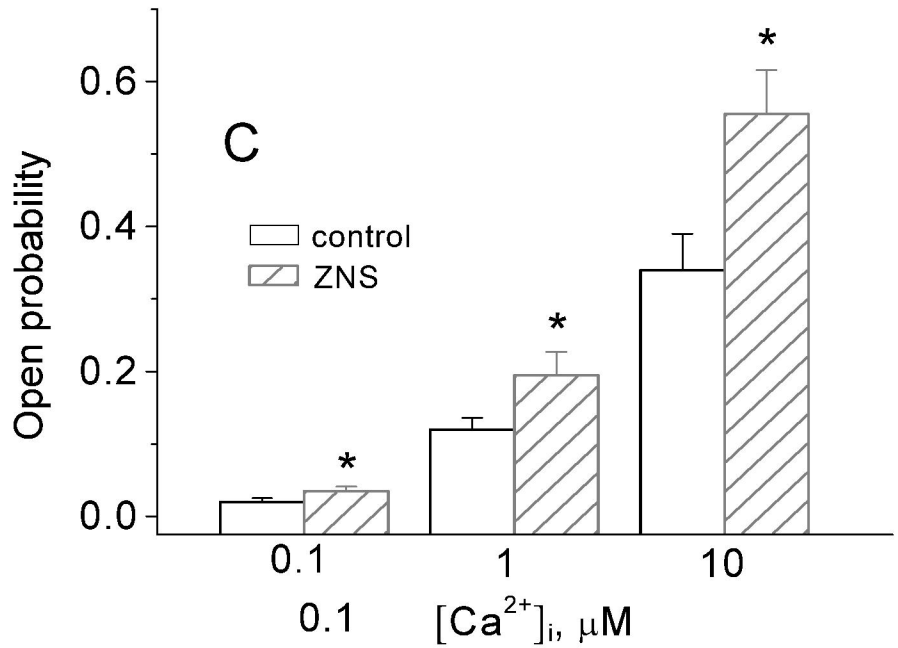
C
Open probability
control
ZNS
*
*
*
0.0
0.2
0.4
0.6
0.1
1
10
0.1
[Ca2+]i, μM

Figure 4

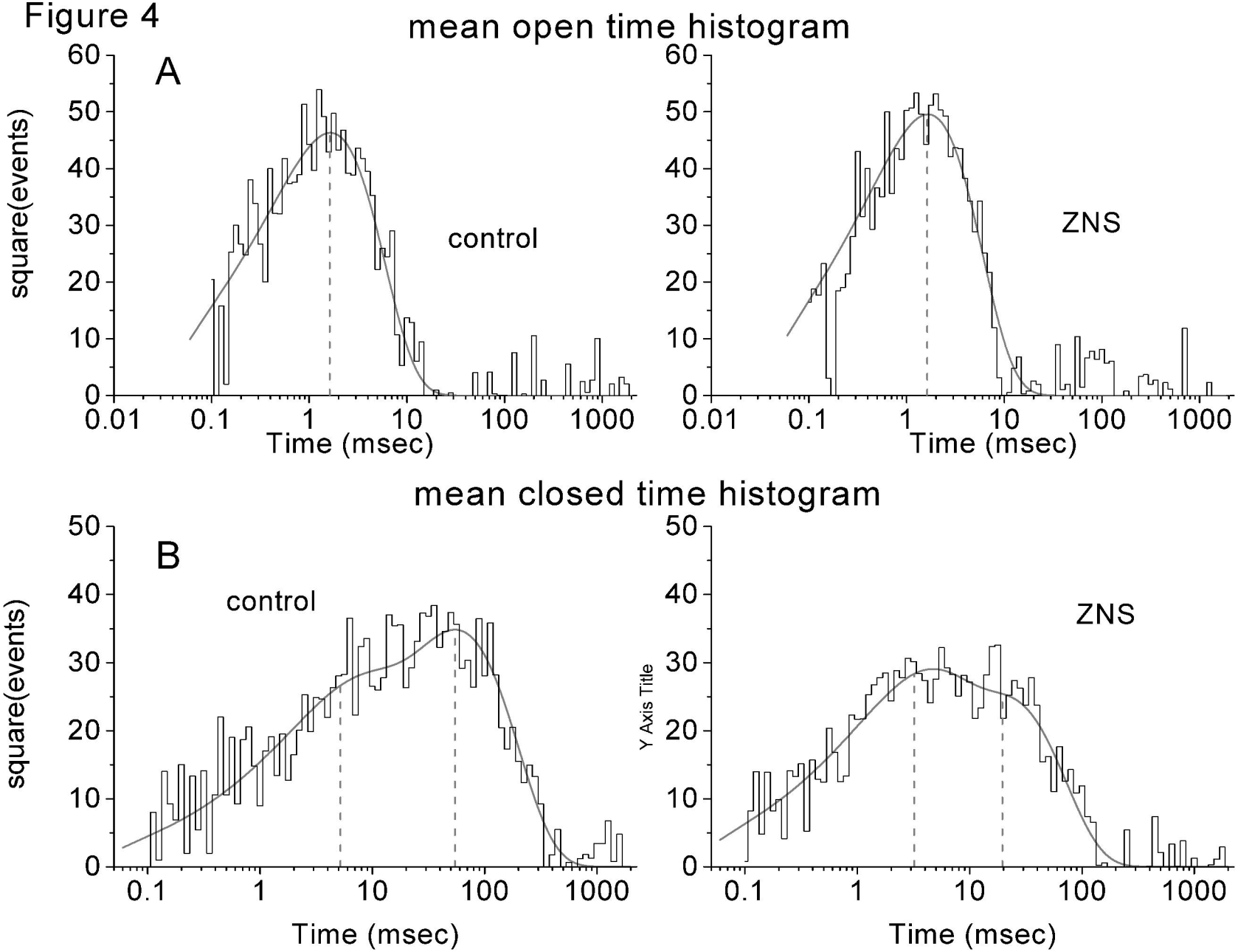
mean open time histogram
A
square(events)
control
ZNS
Time (msec)
mean closed time histogram
B
control
ZNS
Y Axis Title
Time (msec)

Figure 5

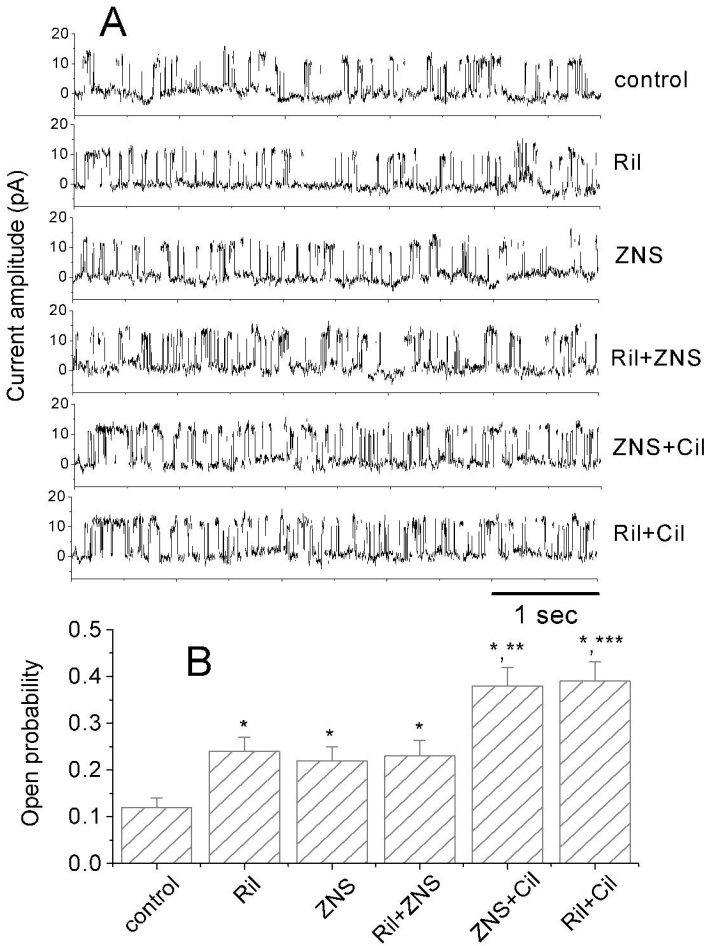
A
Current amplitude (pA)
20
10
0
control
Ril
ZNS
Ril+ZNS
ZNS+Cil
Ril+Cil
1 sec
B
Open probability
0.5
0.4
0.3
0.2
0.1
0.0
*
* **
* ***
control
Ril
ZNS
Ril+ZNS
ZNS+Cil
Ril+Cil

Figure 6

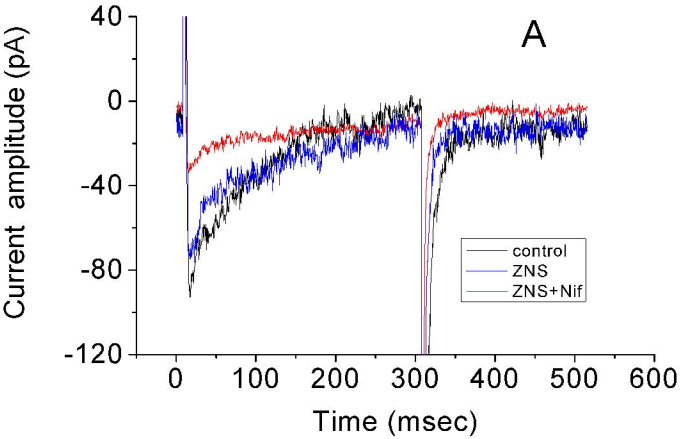
A
Current amplitude (pA)
40
0
-40
-80
-120
0
100
200
300
400
500
600
Time (msec)
control
ZNS
ZNS+Nif

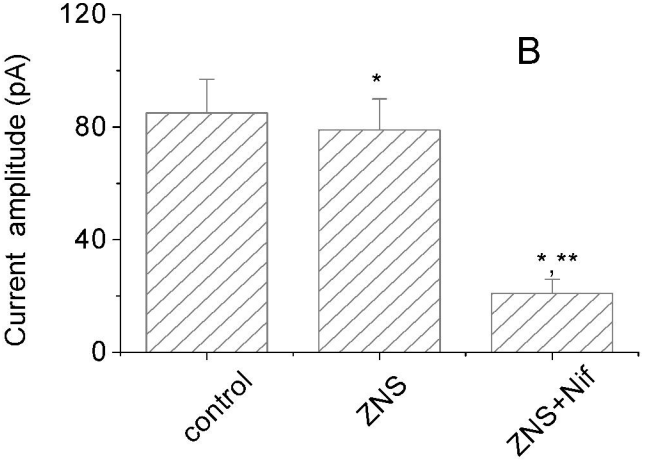
B
Current amplitude (pA)
120
80
40
0
*
* **
control
ZNS
ZNS+Nif

Figure 7

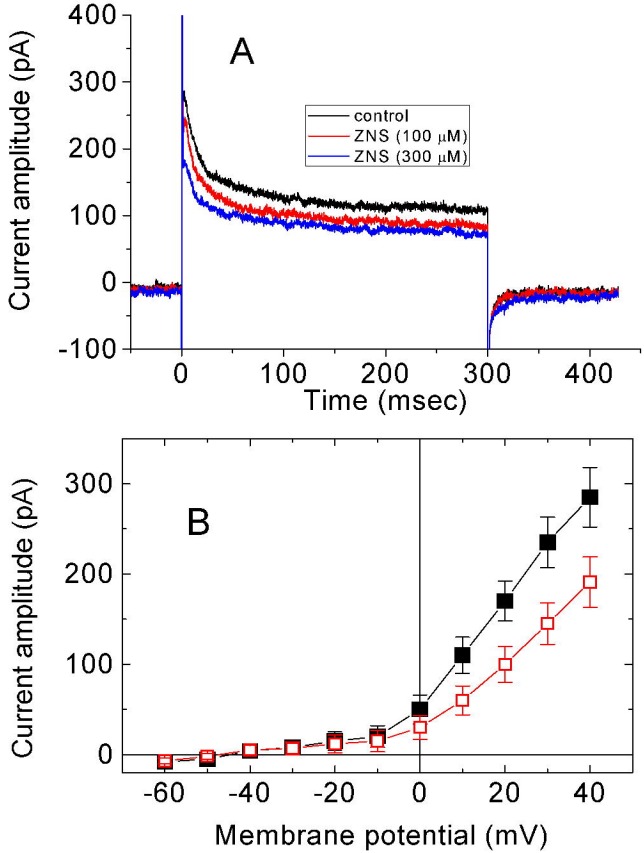
A
control
ZNS (100 μM)
ZNS (300 μM)
Current amplitude (pA)
Time (msec)
400
300
200
100
0
-100
0
100
200
300
400
B
Current amplitude (pA)
Membrane potential (mV)
300
200
100
0
-60
-40
-20
0
20
40

Figure 8

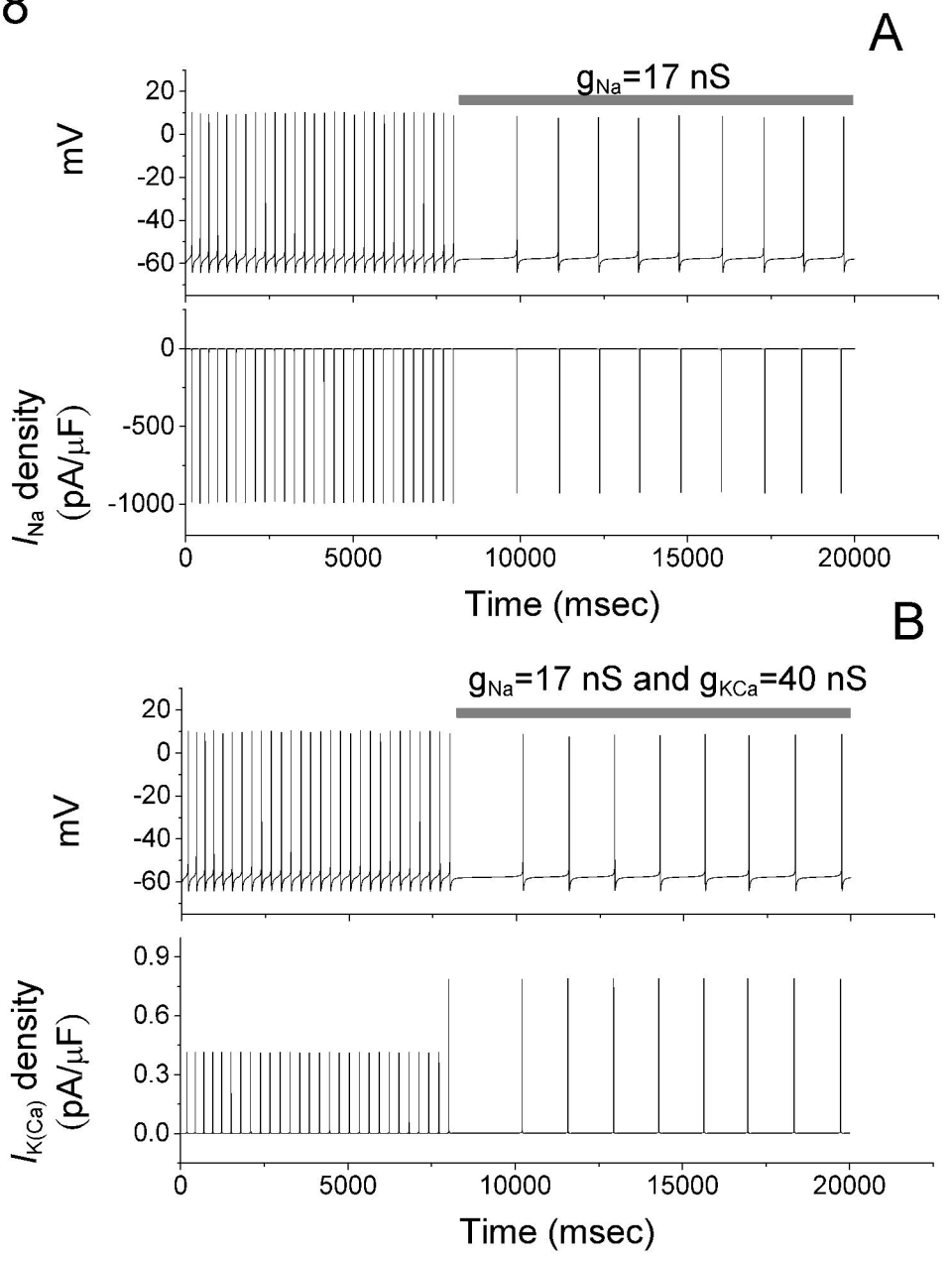
A
g_{Na}=17 nS
mV
20
0
-20
-40
-60
I_{Na} density (pA/μF)
0
-500
-1000
0
5000
10000
15000
20000
Time (msec)
B
g_{Na}=17 nS and g_{KCa}=40 nS
mV
20
0
-20
-40
-60
$I_{K(Ca)}$ density (pA/μF)
0.9
0.6
0.3
0.0
0
5000
10000
15000
20000
Time (msec)